

Dynamic modeling and simulation of inter-shaft bearings with localized defects excited by time-varying displacement

Jing Tian¹, Yan-Ting Ai², Cheng-Wei Fei³, Feng-Ling Zhang² and Yat-Sze Choy⁴

¹School of Power and Energy, Northwestern Polytechnical University, Xi'an, P.R. China

²Liaoning Key Laboratory of Advanced Measurement and Test Technology for Aviation Propulsion System, Shenyang Aerospace University, P.R. China

³Department of Aeronautics and Astronautics, Fudan University, Shanghai, P.R. China

⁴Department of Mechanical Engineering, The Hong Kong Polytechnic University, Kowloon, P.R. China

Corresponding author:

Cheng-Wei Fei, Department of Aeronautics and Astronautics, Fudan University, Shanghai 200433, P.R. China.

Email: cwfei@fudan.edu.cn

Abstract

To accurately describe the dynamic features of inter-shaft bearings with localized defect under operation, the dynamic model of inter-shaft bearing with localized defects was established with respect to time-varying displacement excitation. Based on fault simulations on a birotor experimental rig, the developed dynamic model of inter-shaft bearing is validated to have high accuracy (over 99%) when localized defects happen on inner and outer race with co- and counter-rotation, which indicates that the model can be adopted to simulate the faults of inter-shaft bearing instead of experiment. Through investigation of the square-root (SR) amplitudes of bearing vibration with different defect sizes, radial loads, and rotational directions, we find that the SR amplitudes of bearing vibration increase with increasing defect size and radial load for both co- and counter-rotation. The amplitudes of counter-rotation are larger than those of co-rotation for inner race and outer race, and the amplitude of inner race defect are larger than that of outer race defect for the same defect size or same radial load. This work reveals the SR variation of bearing vibration with localized surface defects under different defect sizes and radial loads, and accurately describes the dynamic characteristics of inter-shaft bearing with localized defects. The efforts of this study open a door to adopt a dynamic model in the future to evaluate and monitor the health condition of inter-shaft bearings in an aeroengine or other rotating machinery.

Keywords

Inter-shaft bearing, time-varying displacement, localized defect, dynamic model, radial loads

1. Introduction

Inter-shaft bearings are widely applied to connect high and low-pressure shafts among birotor or multi-rotor structures of an advanced aeroengine or gas turbine (Fei and Bai, 2013). The inter-shaft bearing has to work in the complex environment of high temperature and is difficult to lubricate (Ai et al., 2017). Therefore, this inevitably leads to damage on the surfaces of both inner race and outer race of an inter-shaft bearing. To ensure the reliability and security of an aeroengine, it is of profound significance for the fault prediction of the bearings to establish the dynamic model of inter-shaft bearings with surface defects and then to achieve early vibration characteristics by simulation analysis (Shah and Patel, 2014; Rai and Upadhyay, 2016).

Dynamic modeling and simulation on rolling bearings with surface defects have been widely investigated from theoretical and experimental perspectives. Sunnersjö (1978) built a four-degrees-of-freedom (DOF) model by adopting a nonlinear spring to be equivalent to rolling balls. But this model is only suitable for the dynamic characteristic analysis of rolling bearings with the emphasis on single transient state. McFadden and Smith (1984) studied a dynamic model of the vibration induced by a single point in the inner race of a rolling element bearing and then gained the vibration features of two faults. Su and Lin (1992) and Su et al. (1993) discussed the dynamic modeling of bearing faults under time-varying loads and

analyzed frequency characteristics under different loads. Patel et al. (2010, 2013, 2014) built a six-DOF dynamic model for the fault simulation and analysis of rolling bearings. Patil et al. (2009, 2010) investigated the effect of defect sizes on vibration characteristics regarding a ball bearing as a nonlinear contracted spring. Kulkarni and Sahasrabudhe (2014) evaluated the influence of defect sizes, locations, and loads on outer race on the responses of ball bearing vibration by simulating the impulse-producing bearing fault based on a cubic Hermite spline on the foundation of Patil's model.

Niu et al. (2017) established a six-DOF damage model of a ball bearing for each component of the bearing by considering various factors such as gyroscopic effect, eccentricity, and lubrication. Dougdag et al. (2012) developed a dynamic model of surface defects on ball bearings and validated the model by static and dynamic simulation experiments. Moazen et al. (2015) proposed a multi-body nonlinear dynamic model for the simulation and analysis of rolling bearing faults. Kankar et al. (2012) studied the influence of crinkles on inner and outer races on the dynamic characteristics of rolling bearings by forming the dynamic model of the crinkle. Kiral and Karagulle (2003) presented a dynamic model of a rolling element bearing based on the finite element method to acquire static and dynamic characteristics. Fei et al. (2014) opened the door to employing information entropy to detect rotor vibration fault quantitatively and achieve efficient signals of rotor vibration. From the above analyses, it is easily found that most studies on the dynamic modeling and simulation analysis of defects focus on general bearings such as the rolling element bearing. Besides, investigations on the dynamic modeling and dynamic characteristics analysis of inter-shaft bearings have not been carried out until now. The objective of this paper is to develop a dynamic model of inter-shaft bearings with localized defects by considering bearing radial clearance, time-varying displacement excitation, and the rotational features of inner race and outer race. With the fault simulations of inter-shaft bearing with localized defects based on a birotor experiment rig, the feasibility and effectiveness of the proposed dynamic model is validated by comparing the results of model simulation with both experiments and theoretical values. Lastly, we investigate the dynamic characteristics of inter-shaft bearing with the defects of both inner race and outer race under co- and counter-rotation of two rotors, based on the proposed dynamic model with respect to different defect sizes and radial loads.

The rest of this paper is organized as follow. The dynamic model of localized defect in inter-shaft bearing is established under the excitation of time-varying displacement in Section 2. Section 3 discusses the experiments on a birotor test bench to simulate the fault of localized defects on inner race and outer race of intershaft bearing with co- and counter-rotation, and then the proposed dynamic model is validated by comparing with the experiment data. In Section 4, the dynamic characteristics of inter-shaft bearing with localized defect are investigated under the effects of different defect sizes and radial loads. Some conclusions of this study are summarized in Section 5.

2. Dynamic modeling

2.1. Simplification of inter-shaft bearing

For a birotor system, inter-shaft bearings are adopted to connect the two shafts. The two rotors in the bearing, the inner race and outer race, simultaneously rotate with high- and low-pressure rotors, following either coor counter-rotation. The rotational speed of the bearing is determined by the difference of the rotational speeds of two rotors. A diagram of inter-shaft bearing is shown in Figure 1. The inter-shaft bearing of an aeroengine is usually a cylindrical roller bearing. When the rollers do not slip, the localized faults can be established as a four-DOF dynamic model based on Hertz contact theory (Shao et al., 2014; Liu and Shao, 2015). Based on Patil's hypothesis, the contact between roller and raceway can be simplified as a nonlinear spring– mass system.

2.2. Hertz contact force

In line with Hertz contact theory (Shao et al., 2014; Liu and Shao, 2015), Harris et al. (2001) give the relationship between nonlinear loads and displacement as follows:

$$F = K\delta^n \quad (1)$$

where K is the deformation coefficient of the loads and δ denotes the radial displacement. Generally, a cylindrical roller bearing has $n=10/9$ and a ball bearing has $n=3/2$ (Harris et al., 2001).

The total deformation between two races is defined as the sum of normal deformations between two races and rolling elements, i.e.,

$$\delta = \delta_i + \delta_o \quad (2)$$

In light of equations (1) and (2), K is obtained as

$$K = \frac{F}{\delta^n} = \frac{F}{(\delta_i + \delta_o)^n} = \left[\frac{1}{\frac{\delta_i}{F^{1/n}} + \frac{\delta_o}{F^{1/n}}} \right]^n = \left[\frac{1}{\left(\frac{1}{K_i}\right)^{1/n} + \left(\frac{1}{K_o}\right)^{1/n}} \right]^n \quad (3)$$

in which δ_i and δ_o are the deformations on normal direction between both the inner and outer races and the roller, respectively; K_i and K_o indicate the contact stiffness between both the inner and outer races and the roller, respectively. For a cylindrical roller bearing, $K = 8.06 \times 10^4 l^{0.8}$, where l is the length of the rollers (Shao et al., 2014).

The reduced model of inter-shaft bearing investigated in this paper is shown in Figure 2. When H_d is time-varying displacement excitation as the roller passes a defect, the deformation δ is

$$\delta = (x_o - x_i) \cos \theta_j + (y_o - y_i) \sin \theta_j - C_r - H_d \quad (4)$$

where x_o and y_o , respectively, are the displacements of the outer race center along the x - and y -axes, θ_j is the intersection angle between the j th roller and the x -axis, x_i and y_i , respectively, are the displacements of the inner race center along the x - and y -axes, and C_r is the initial radial clearance between roller and race. In equation (4),

$$\theta_j = \omega_c t + \frac{2\pi(j-1)}{Z} + \theta_{t0} \quad (5)$$

with

$$\omega_c = \frac{1}{2} \left[\omega_i \left(1 - \frac{d}{D_m} \cos \alpha \right) + \omega_o \left(1 + \frac{d}{D_m} \cos \alpha \right) \right] \quad (6)$$

in which ω_i , ω_o , and ω_c are, respectively, the angular velocities of the inner race, outer race, and roller of inter-shaft bearing, θ_{t0} denotes the initial intersection angle of the first roller with respect to the x -axis; Z indicates the number of rolling elements, d denotes the diameter of rollers, D_m explains the pitch diameter of the bearing, and α implies bearing pressure angle. Inputting equation (4) into equation (1), the Hertz contact force of the j th roller is

$$F_j = K[(x_o - x_i) \cos \theta_j + (y_o - y_i) \sin \theta_j - C_r - H_d]^{10/9} \quad (7)$$

Thus, the component forces of the Hertz contact force in the directions of the x - and y -axes are expressed by

$$\left\{ \begin{array}{l} F_X = K \sum_{j=1}^Z [(x_o - x_i) \cos \theta_j + (y_o - y_i) \sin \theta_j - C_r - H_d]^{10/9} \cos \theta_j \\ F_Y = K \sum_{j=1}^Z [(x_o - x_i) \cos \theta_j + (y_o - y_i) \sin \theta_j - C_r - H_d]^{10/9} \sin \theta_j \end{array} \right. \quad (8)$$

2.3. Excitation of time-varying displacement

This study focuses on the early outer race defect of an inter-shaft bearing and the radial length of the defect which is larger than that of cylindrical rollers. This fault has smaller width than the diameter of roller (rolling elements) so that the displacement of the declined roller is less than the defect depth when the roller goes through the defect. The status of a roller passing defect is illustrated in Figure 3. Herein, H_d is the displacement of the roller as passing the defect, H is the defect depth, B is the defect width, and H_e is the largest displacement excitation. As illustrated in Figure 3, the roller always contacts edge I of the defect when the roller approaches and passes the defect, and is away from the defect region as it passes edge II of the defect. The time-varying displacement of the roller passing the defect can be described by a half-sine function. The maximum displacement excitation H_e is expressed as

$$H_e = \frac{d}{2} - \sqrt{\left(\frac{d}{2}\right)^2 - \left(\frac{B}{2}\right)^2} \quad (9)$$

When the roller passes the defect, the excitation function of time-varying displacement is expressed as

$$H_d = \begin{cases} \begin{cases} H_e \sin(\pi/\phi_d) \\ \cdot (\theta_j - \theta_d) \end{cases} & \begin{cases} 0 \leq (\text{mod}(\theta_j - \theta_d, 2\pi)) \leq \phi_d \text{ or} \\ -2\pi \leq (\text{mod}(\theta_j - \theta_d, 2\pi)) \\ \leq -2\pi + \phi_d \\ \text{other} \end{cases} \\ 0 & \end{cases} \quad (10)$$

where mod is the solution of the sine function, ϕ_d is the angle of defect, θ_{d0} indicates the initial position of defect with respect to the x -axis at $t = 0$, which is illustrated in Figure 4, and θ_d indicates the intersection angle between edge I and edge II on the defect. When the defect is located on the inner race, the intersection angle θ_d is described as

$$\theta_d = \omega_i t + \theta_{d0} \quad (11)$$

When the defect is located on the outer race, the intersection angle θ_d is described as

$$\theta_d = \omega_o t + \theta_{d0} \quad (12)$$

2.4. Kinetic differential equation

Based on the hypothesis of a rigid ring (Ni and Deng, 2009), inter-shaft bearing is modeled as a four-DOF dynamic system. In line with the contact stiffness K , the damping c , the Hertz contact force F , the time-varying displacement x , and the constant radial load W , the kinetic differential equation of dynamic system is gained as

$$\begin{cases} M_o \ddot{x}_o + c \dot{x}_o + K \sum_{j=1}^Z \lambda \delta^{109} \cos \theta_j = W + F_o \cos(\omega_o t) \\ M_o \ddot{y}_o + c \dot{y}_o + K \sum_{j=1}^Z \lambda \delta^{109} \sin \theta_j = F_o \sin(\omega_o t) \\ M_i \ddot{x}_i + c \dot{x}_i - K \sum_{j=1}^Z \lambda \delta^{109} \cos \theta_j = W + F_i \cos(\omega_i t) \\ M_i \ddot{y}_i + c \dot{y}_i - K \sum_{j=1}^Z \lambda \delta^{109} \sin \theta_j = F_i \sin(\omega_i t) \end{cases} \quad (13)$$

Where M_i and M_o are the masses of outer race and inner race, F_i and F_o are the eccentric loads of outer race and inner race, W is the radial load affecting the bearing, and l is the switching value whether rollers and races are contacted, expressed by

$$\lambda = \begin{cases} 1 & \delta > 0 \\ 0 & \delta \leq 0 \end{cases} \quad (14)$$

The improved Newmark-b method (Fleissner et al., 2007; Garza and Millwater, 2015) is applied for the solution of kinetic differential equation and has second order accuracy as $c = 1/2$ and $b = 1/4$ (Zheng and Hasebe, 2000), which is an unconditional stability method.

3. Model validation

3.1. Experimental system

To validate the accuracy of the developed model, the birotor experimental system shown in Figure 5 was employed to simulate the localized defects of an intershaft bearing and acquire its fault data. Meanwhile, the experimental rig simulates the supporting scheme of an advanced aeroengine. In the experimental system, the bearing used is a cylindrical roller bearing (model no. SKF nu1004M), in which the fourth supporting point is regarded as inter-shaft bearing. Four PCB acceleration sensors are located on the bearing pedestal and casing to measure and collect vibration data of the inter-shaft bearing in the x- and y-directions. The distribution of sensors and data acquisition system are displayed in Figure 6. The data obtained are employed to test the analytical results of the proposed dynamic model. Besides, by using a wire-electrode cutting method, a surface defect is produced on the outer race in which the shape of the defect is indicated by the red arrow in Figure 7.

3.2. Parameters of inter-shaft bearing

In a co-rotation experiment of high- and low-pressure rotors, it was set that the revolving speeds of the high and low-pressure rotors are 1000 r/min and 625 r/min, respectively, and the radial load was 200 N. The measured rotation speeds of the high- and low-pressure shafts were 1001 r/min and 624 r/min, respectively. The parameters of the SKF nu1004M bearing are listed in Table 1.

In light of the theory and empirical formula of bearing fault frequency in the literature (McInerny and Dai, 2003; Ma and Liao, 2014; Wang et al., 2014), for coand counter-rotation of inner race and outer race, the fault frequencies of surface defect of inter-shaft bearing are as listed in Table 2.

3.3. Validation of dynamic model

Owing to structural features of the inter-shaft bearing, fault signals simulated in the experimental rig are transmitted into pedestal and casing from the sources of signals by a complex transmission path (Fei et al., 2018). Thus, it is unavoidable in this path that some noise is overlaid on the original signals so that the collected signals of bearing vibration contain some noise. To reduce the influence of noise, the multi-scale morphological filtering method (Li et al., 2011) and wavelet denoising method (Kim et al., 2001) were utilized to de-noise the acquired fault signals. Then, the time-domain signals and the envelope spectrum of outer race fault are as depicted in Figure 8.

As shown in Figure 8(a), when the outer race of the inter-shaft bearing has a defect, the time signal of this defect has an obvious impact phenomenon and the shock pulses exhibit periodical change. The periodical impact phenomenon is caused by the effect of the rotating frequencies of shaft or holder on the impacts produced as rollers pass the defect. As shown in Figure 8(b), the passing frequency of rollers going through outer race is 33.02 Hz and has an error of 0.53 Hz relative to theoretical value 33.55 Hz in Table 2. Perhaps the reason is that the bearing slips in experiment and the slip appears as second harmonic and third harmonic frequencies of the passing frequency.

When the defect is located on the outer race of the inter-shaft bearing, based on the established dynamic model the time-domain signals and the envelope spectrum of outer race fault in the inter-shaft bearing are as illustrated in Figure 9.

As revealed in Figure 9(a), the time-domain signals of bearing vibration also hold obvious periodical impact components. Figure 9(b) illustrates that the envelop spectrum gained from model simulation contains 1–4 multiple frequencies of the passing frequency and the amplitudes of the signals reduce progressively, which are basically consistent with that obtained

from experiment. The passing frequency based on the model is 33.57 Hz, which is almost equal to the theoretical value, 33.55 Hz. Therefore, the developed dynamic model of localized defect in inter-shaft bearing is verified to be efficient and precise, because it is able to more accurately describe the dynamic characteristics of inter-shaft bearing with localized defects than the experiments on birotor simulation test rig.

Figure 10 shows the envelope spectrum of the experimental and simulation signals with co-rotation, when the defect is located on the inner race of the inter-shaft bearing. As shown in Figure 10(a), the experimental envelope spectrum contains multiples of the passing frequency of the inner race fault. Although the signal contains a lot of noise, the fault frequency is obvious. Comparing Figure 10(a) and (b), we find that the results of the dynamic model are basically consistent with the experimental results. The experimental model and the dynamic model contain the same trend of the fault frequency, and the amplitude decreases with the increasing multiplier frequency. The fault frequency calculated by the dynamic model is 47.76 Hz, and the fault frequency measured by experiment is 47.21 Hz. The error is only about 1%, which proves that the dynamic model developed in this paper can effectively and accurately simulate the inner ring fault of the intershaft bearing.

To further support the effectiveness of the developed dynamic model, four working conditions of co- and counter-rotation with respect to inner race defect and outer race defect are evaluated. From the analyses, the envelope spectra of the four cases are shown in Figures 10 and 11.

As revealed in Figures 10 and 11, the fault frequencies of four defects are clearly simulated including frequency features of fault signal on original frequency, double frequency, and triple frequency. With respect to the theoretical values in Table 2, the errors of fault frequency based on dynamic model are less than 1%. Therefore, the proposed dynamic model is again verified to achieve high accuracy in describing the dynamic characteristics of an inter-shaft bearing with localized defects. Additionally, it is also seen that the (acceleration) amplitudes of envelope spectra for inner race defects are greater than outer race defects, and those of counter-rotation are higher than co-rotation with respect to the same order of frequency.

4. Simulation of dynamic characteristics of inter-shaft bearings

The excellent performance of the developed dynamic model has been validated in the above section. In this section, we investigate the dynamic characteristics of an inter-shaft bearing with numerous localized defects and radial loads to achieve precise information for performance evaluation and health monitoring of an inter-shaft bearing.

4.1. Effect of defect size on vibration of intershaft bearing

The square root (SR) amplitude of a signal reflects the energy magnitude of this signal (Pachaud et al., 1997) and can be used to assess the degree of the bearing fault and the stability of the fault. A slight fault has a small impact on the SR value. The SR value becomes large with increasing impact energy. Thus, the SR value of signal amplitude is used in this paper to evaluate the damage degree of bearing faults. The SR formula is as follows:

$$X_r = \left(\frac{1}{N} \sum_{k=1}^N \sqrt{|x(k)|} \right)^2 \quad (15)$$

where N is number of sampling points and x(k) is vibration amplitude of the sampling point.

Based on the built dynamic model, the SR values of fault signals of an inter-shaft bearing affected by the radial load of 300N are discussed when the variation of defect size is from 0.1mm to 2mm with the interval of 0.1 mm. For the conditions of co- and counter-rotation, therefore, the SR variations of vibration signals for inner race defects and outer race defects are obtained, as shown in Figure 12.

4.2. Effect of radial loads on vibration of inter-shaft bearing

This subsection reports the effect of radial loads on the vibration of an inter-shaft bearing. A defect size 0.5mm is selected as the objective of study. In terms of the established dynamic model, with the variation of radial loads the SR changes of bearing vibration signals on the inner and outer race defects with co- and counter- rotation are shown in Figure 13.

4.3. Discussion

Through the research of the vibration features of intershaft bearing with localized defects affected by different

defect sizes and radial loads, some results can be achieved as follows: As revealed in Figure 12, for both co- and counterrotation between inner race and outer race, the SR values of vibration signals increase with the increase of defect size, which indicates that the energy of vibration for bearing increases with increasing size of defect. The reason is that the increase of defect size enhances the SR of vibration amplitude and then increases impact energy when the roller passes the defect. For the same size of bearing defect, the SR value of vibration for counterrotation is larger than that of co-rotation, resulting from the fact that the rollers pass the defect more frequently and its impact energy is larger during the same time when inner race and outer race reversely rotate. In addition, we also find the phenomenon that the SR value for inner race defect is larger than that for outer race defect when they have the same defect. This is because the impact number (or passing frequency) of the defect on inner race is larger than that on outer race in the same time due to the smaller radius for inner race versus outer race. The SR amplitude exhibits a growing trend as the fault size increases in co-rotation, but it is relatively stable with respect to the counter-rotation. The reason is that the speed discrepancy between inner race and outer race is relatively small with the fault passing frequency of 33.57 Hz. When the fault size increases, the fault depth does not increase too much and the fault frequency is low. Thus, the change of impact energy is not large due to the relative stable SR value. For counter-rotation, larger speed discrepancy between the inner race and outer race causes more impacts, larger impact energy, and more obvious fault.

As indicated in Figure 13, the SR values of bearing vibration have the increasing trend with the rise of radial loads, for the co-rotation and counter-rotation of inter-shaft bearing, because the rise of radial loads enlarges the energy of impact as rollers go through the defect. Besides, the SR value of bearing vibration for counter-rotation is larger than that for co-rotation. The reason is that the passing frequency for counterrotation is higher than for co-rotation, so that the impact frequency between roller and surface defect is higher for counter-rotation, and thereby the SR value of bearing vibration for an inner race defect is larger than that for an outer race defect. Besides, the increasing trend of SR value of both co- and counterrotation is more obvious with the increase of load than the size. This is due to the change of the vibration caused by the size change is not very obvious, but the increase of the load on the impact energy is more prominent.

In conclusion, the change of the SR amplitude of bearing vibration with localized surface defects is acquired with the variations of defect size and radial load, which accurately reflects and describes the dynamic characteristics of inter-shaft bearing with localized defect on inner race and outer race. These results cater for engineering practice, which further support the effectiveness and feasibility of the developed dynamic model in the simulation of inter-shaft bearing faults. The efforts of this study open a door to evaluate and monitor the health condition of inter-shaft bearings in an aeroengine using the dynamic model.

5. Conclusions

The aim of this paper was to develop an efficient dynamic model of localized defects in an inter-shaft bearing with respect to time-varying excitation of displacement, and to accurately simulate and describe the dynamic characteristics of an inter-shaft bearing with localized defects. Through the validation of the developed model and the investigation on the dynamic characteristics of inter-shaft bearing with localized defects based on the developed model, some conclusions are summarized as follows:

1. Through the study on validation of the dynamic model by comparison with experiment on a birotor simulation test rig, it is indicated that the developed model has higher computational accuracy in acquiring impact responses (timedomain signals and envelope spectrum of localized defect on outer race of inter-shaft bearing), which is almost consistent with the theoretical values.
2. As shown in the investigation on the dynamic responses of the inner and outer race defects of inter-shaft bearing with co-rotation and counterrotation, the developed model achieves an error of less than 1% and high modeling precision referring to the theoretical values.
3. From the simulation of dynamic characteristics of inter-shaft bearing by regarding different defect sizes and numerous radial loads, we find that (i) with the increase of defect size or radial load, the square-root (SR) amplitude of bearing vibration with inner and outer race defects enlarges for co-rotation or counter-rotation; (ii) for a same fault or load, the SR amplitudes of bearing vibration for co-rotation is smaller than these for counter-rotation; (iii) for a same defect size or radial load, the SR amplitudes of inner race are greater than these of outer race for inter-shaft bearing.

The SR change of bearing vibration with regard to different defect size and radial loads are acquired, which accurately describe the dynamic characteristics of inter-shaft bearing with localized defect on inner race and outer race with co-rotation and counter-rotation referencing experiment results and theoretical values. The achievements cater for engineering practice, which full support the effectiveness and feasibility of the developed dynamic model in simulating inter-shaft bearing faults. The efforts of this study provide a useful insight to adopt a dynamic model to evaluate and monitor the health condition of inter-shaft bearing in an aeroengine or other rotating machinery.

Acknowledgements

The authors would like to thank the organizations that provided funding for this work.

Declaration of Conflicting Interests

The author(s) declared no potential conflicts of interest with respect to the research, authorship, and/or publication of this article.

Funding

The author(s) disclosed receipt of the following financial support for the research, authorship and/or publication of this article: This work was supported by the National Natural Science Foundation of China (grant numbers 11702177 and 51605016), the Natural Science Foundation of Liaoning Province of China (grant number 20180550650), and Research Start up Funding of Fudan University.

ORCID iD

Jing Tian <http://orcid.org/0000-0002-1904-1473>

References

- Ai YT, Guan JY, Fei CW, et al. (2017) Fusion information entropy method of rolling bearing fault diagnosis based on n-dimensional characteristic parameter distance. *Mechanical Systems and Signal Processing* 88(3): 123–136.
- Dougdag M, Ouali M, Boucherit H, et al. (2012) An experimental testing of a simplified model of a ball bearing: stiffness calculation and defect simulation. *Meccanica* 47(2): 335–354.
- Fei CW and Bai GC (2013) Wavelet correlation feature scale entropy and fuzzy support vector machine approach for aeroengine whole-body vibration fault diagnosis. *Shock and Vibration* 20(2): 341–349.
- Fei CW, Bai GC, Tang WZ, et al. (2014) Quantitative diagnosis of rotor vibration fault using process power spectrum entropy and support vector machine method. *Shock and Vibration* 2014: 957531.
- Fei CW, Choy YS, Tang WZ, et al. (2018) Multi-feature entropy distance approach with vibration and AE signals for process feature extraction and diagnosis of rolling bearing faults. *Structural Health Monitoring* 17(2): 156–168.
- Fleissner F, Gaugele T and Eberhard P (2007) Applications of the discrete element method in mechanical engineering. *Multibody System Dynamics* 18: 81–94.
- Garza J and Millwater H (2015) Multicomplex newmark-beta time integration method for sensitivity analysis in structural dynamics. *AIAA Journal* 53(5): 1188–1198.
- Harris TA, Barnsby RM and Kotzalas MN (2001) A method to calculate frictional effects in oil-lubricated ball bearings. *Tribology Transactions* 44(4): 704–708.
- Kankar PK, Sharma SC and Harsha SP (2012) Nonlinear vibration signature analysis of a high speed rotor bearing system due to race imperfection. *Journal of Computational and Nonlinear Dynamics* 7(1): 11014.
- Kim YY, Hong JC and Lee NY (2001) Frequency response function estimation via a robust wavelet de-noising method. *Journal of Sound and Vibration* 244(4): 635–649.
- Kiral Z and Karagüç İle H (2003) Simulation and analysis of vibration signals generated by rolling element bearing with defects. *Tribology International* 36(9): 667–678.
- Kulkarni PG and Sahasrabudhe AD (2014) A dynamic model of ball bearing for simulating localized defects on outer race using cubic hermite spline. *Journal of Mechanical Science and Technology* 28(9): 3433–3442.
- Li B, Zhang PL, Wang ZJ, et al. (2011) Gear fault detection using multi-scale morphological filters. *Measurement* 44(10): 2078–2089.
- Liu J and Shao Y (2015) A new dynamic model for vibration analysis of a ball bearing due to a localized surface defect considering edge topographies. *Nonlinear Dynamics* 79(2): 1329–1351.
- Ma ZG and Liao MF (2014) Local fault detection of intershaft bearing in aircraft engines. *Water, Air & Soil Pollution* 225(8): 1–12.
- Mcfadden PD and Smith JD (1984) Model for the vibration produced by a single point defect in a rolling element bearing. *Journal of Sound and Vibration* 96(1): 69–82.
- McInerney SA and Dai Y (2003) Basic vibration signal processing for bearing fault detection. *IEEE Transactions on Education* 46(1): 149–156.
- Moazen A, Petersen D and Howard C (2015) A nonlinear dynamic vibration model of defective bearings: the importance of modelling the finite size of rolling elements. *Mechanical Systems and Signal Processing* 52–53: 309–326.
- Ni YG and Deng SE (2009) The research on the load distribution in flexible supported bearings based on finite element analysis. In: *The 3rd international conference on mechanical engineering and mechanics*, Beijing, China, 21–23 October 2009, pp. 460–463.
- Niu L, Cao H and Xiong X (2017) Dynamic modeling and vibration response simulations of angular contact ball bearings with ball defects considering the three-dimensional motion of balls. *Tribology International* 109: 26–39.
- Pachaud C, Salvetat R and Fray C (1997) Crest factor and kurtosis contributions to identify defects inducing periodical impulsive forces. *Mechanical Systems and Signal Processing* 11(6): 903–916.
- Patel VN, Tandon N and Pandey RK (2010) A dynamic model for vibration studies of deep groove ball bearings considering single and multiple defects in races. *Journal of Tribology* 132(4): 041101.
- Patel VN, Tandon N and Pandey RK (2013) Vibration studies of dynamically loaded deep groove ball bearings in presence of local defects on races. *Procedia Engineering* 64: 1582–1591.

- Patel VN, Tandon N and Pandey RK (2014) Vibrations generated by rolling element bearings having multiple local defects on races. *Procedia Technology* 14: 312–319.
- Patil MS, Mathew J, Rajendrakumar PK, et al. (2009) An analytical model to predict the effect of localised defect on vibrations associated with ball bearing. *International Journal of Engineering Systems Modelling and Simulation* 1(4): 242–252.
- Patil MS, Mathew J, Rajendrakumar PK, et al. (2010) A theoretical model to predict the effect of localized defect on vibrations associated with ball bearing. *International Journal of Mechanical Sciences* 52(9): 1193–1201.
- Rai A and Upadhyay SH (2016) A review on signal processing techniques utilized in the fault diagnosis of rolling element bearings. *Tribology International* 96: 289–306.
- Shah DS and Patel VN (2014) A review of dynamic modeling and fault identifications methods for rolling element bearing. *Procedia Technology* 14: 447–456.
- Shao Y, Liu J and Ye J (2014) A new method to model a localized surface defect in a cylindrical roller-bearing dynamic simulation. *Proceedings of the Institution of Mechanical Engineers Part J: Journal of Engineering Tribology* 228(2): 140–159.
- Su YT and Lin SJ (1992) On initial fault detection of a tapered roller bearing: frequency domain analysis. *Journal of Sound and Vibration* 155(1): 75–84.
- Su YT, Lin MH and Lee MS (1993) The effects of surface irregularities on roller bearing vibrations. *Journal of Sound and Vibration* 165(3): 455–466.
- Sunnersjö, CS (1978) Varying compliance vibrations of rolling bearings. *Journal of Sound and Vibration* 58(3): 363–373.
- Wang TY, Liang M, Li JY, et al. (2014) Rolling element bearing fault diagnosis via fault characteristic order analysis. *Mechanical Systems and Signal Processing* 45(1): 139–153.
- Zheng T and Hasebe N (2000) Nonlinear dynamic behaviors of a complex rotor-bearing system. *Journal of Applied Mechanics* 67(3): 485–495.

Figures

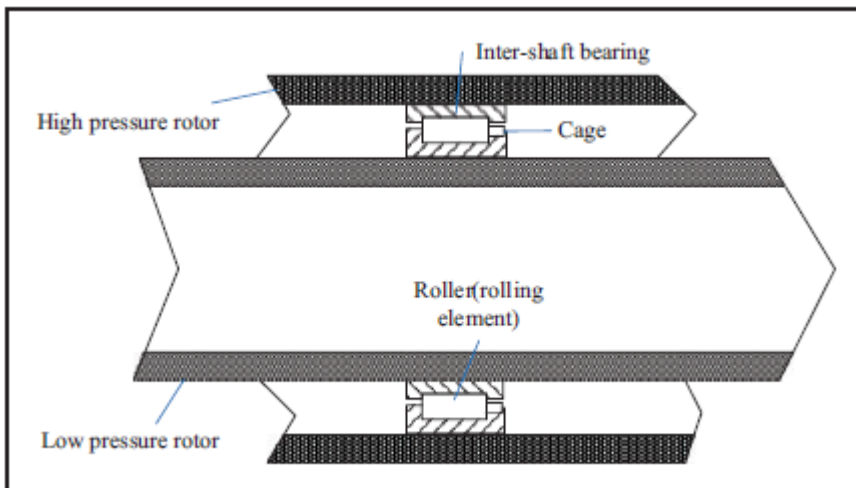


Figure 1. Diagram of an inter-shaft bearing.

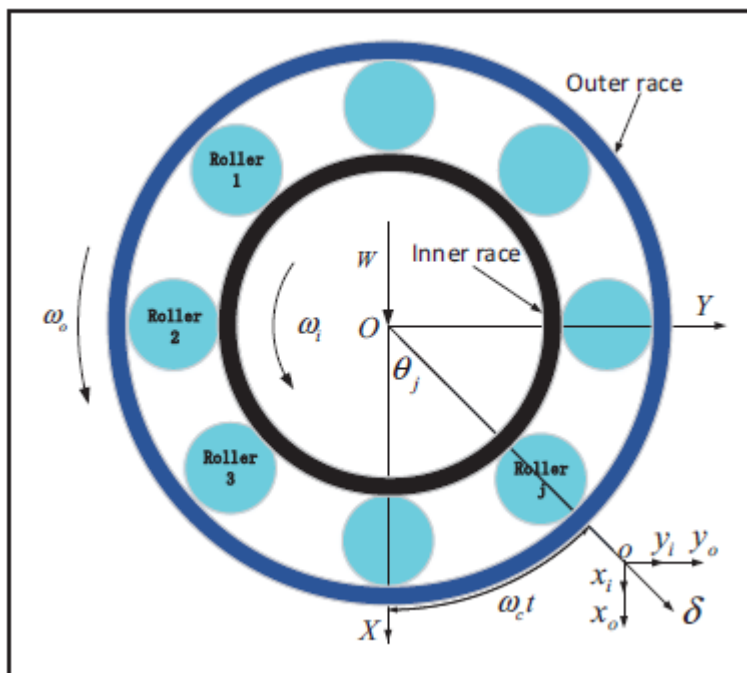


Figure 2. Reduced model of an inter-shaft bearing.

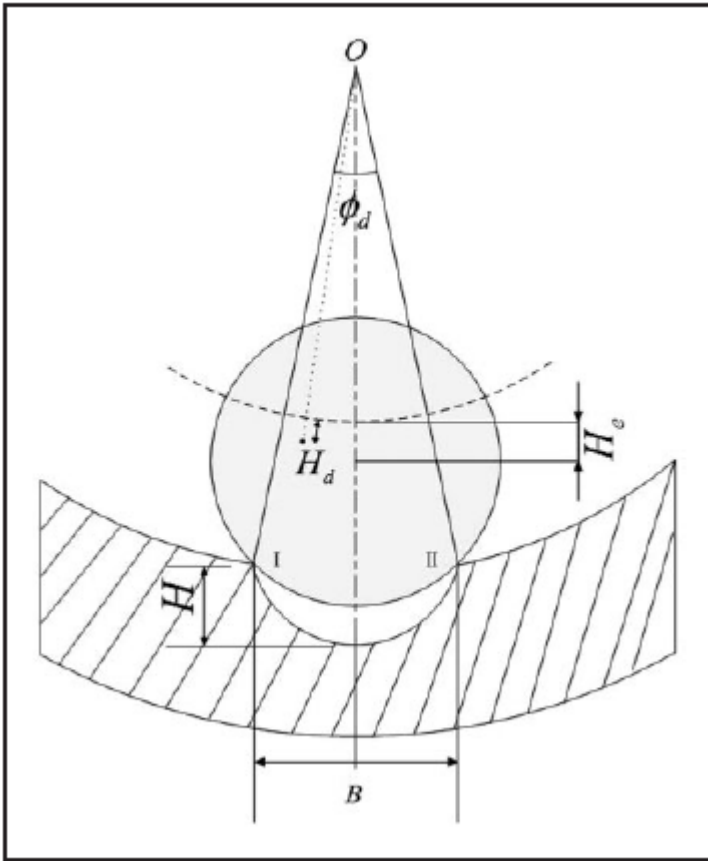


Figure 3. The state diagram of the roller passing a defect. outer race.

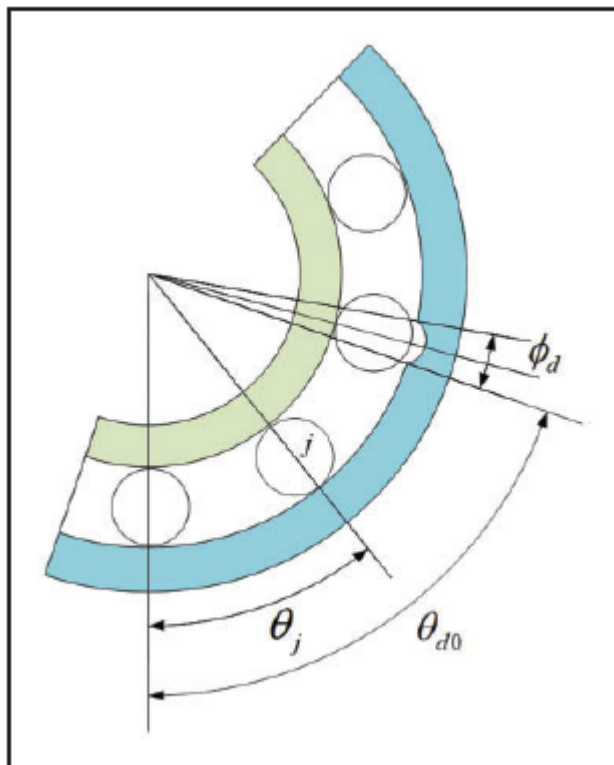


Figure 4. Sketch map of a localized defect on the surface of the

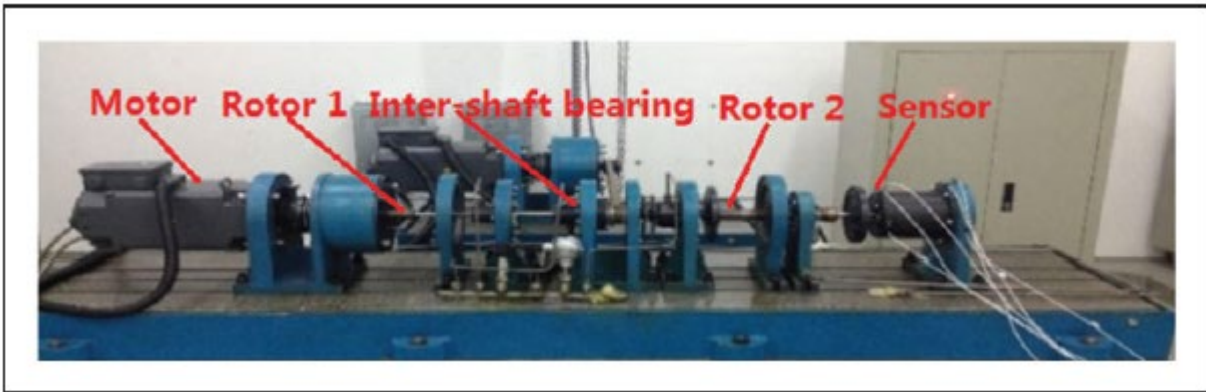


Figure 5. Fault simulation system of birotor inter-shaft bearing.



Figure 6. Distributions of vibration sensors (left) and data acquisition system (right).

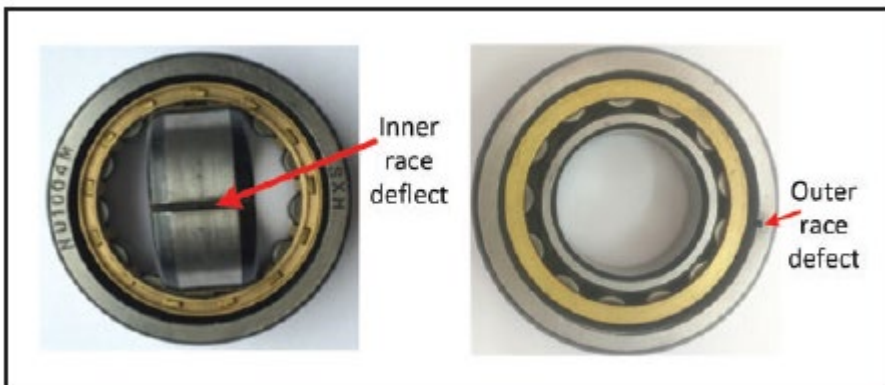


Figure 7. Localized defects on the inner race and outer race of an inter-shaft bearing.

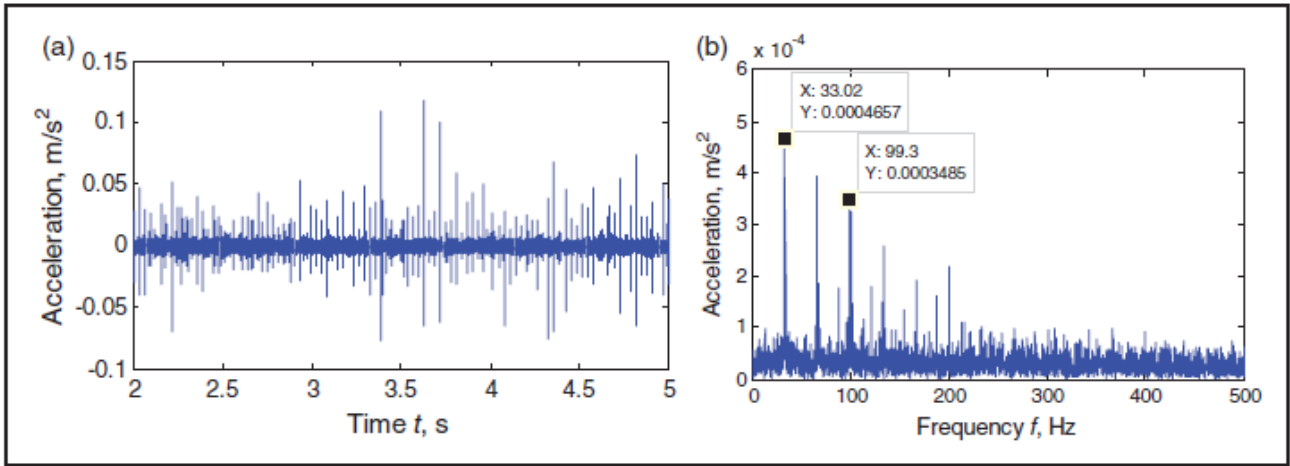


Figure 8. (a) Time-domain signal and (b) envelope spectrum of an outer race defect with co-rotation based on experiment.

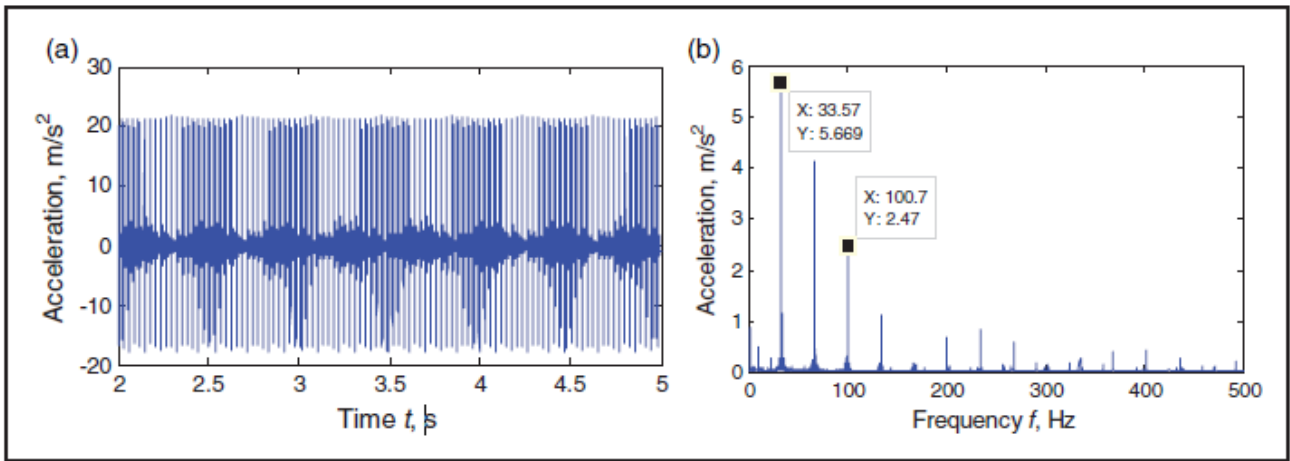


Figure 9. (a) Time-domain signal and (b) envelope spectrum of outer race defect signals with co-rotation based on the model.

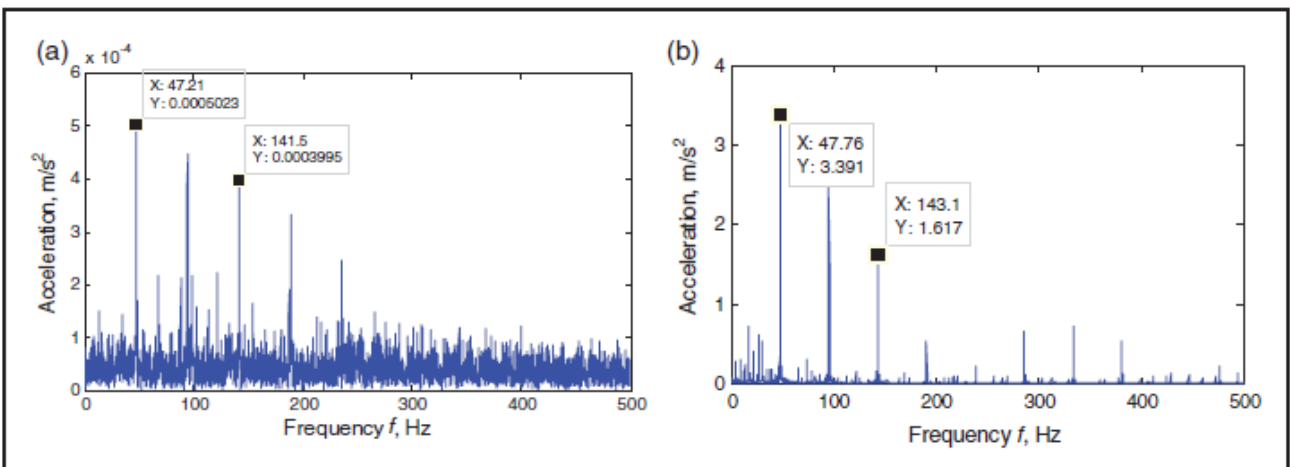


Figure 10. Envelope spectra of inner race defect with co-rotation from (a) experiment and (b) simulation.

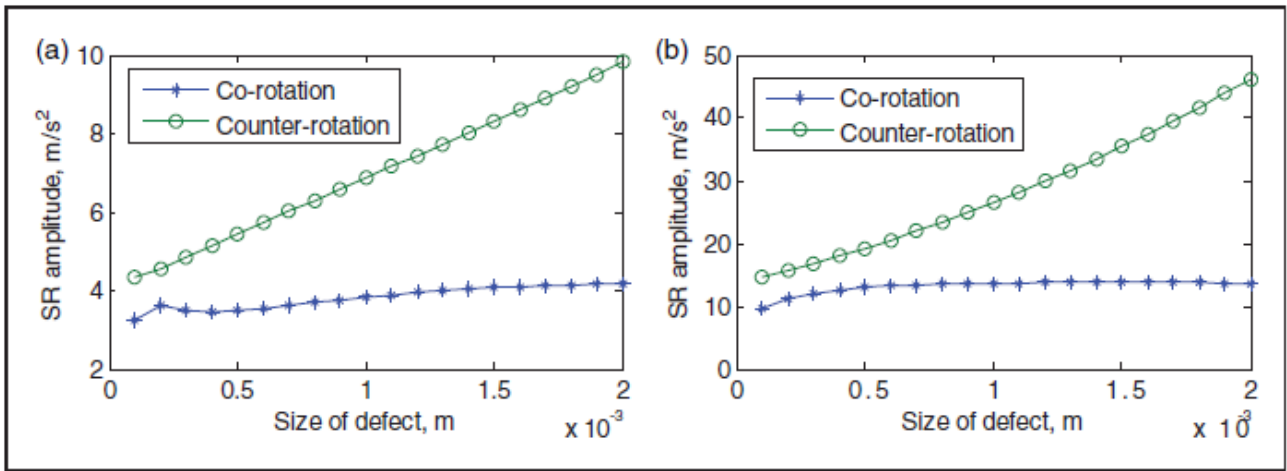


Figure 11. Envelope spectra of (a) outer and (b) inner race defect signals with counter-rotation.

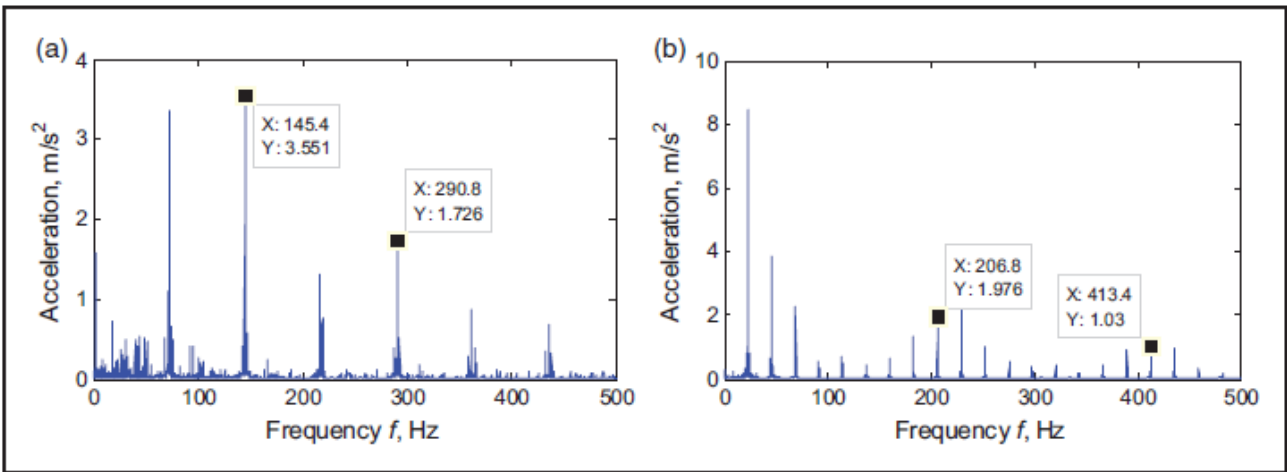


Figure 12. SR variations of bearing vibration signals under different sizes of (a) outer and (b) inner race defects.

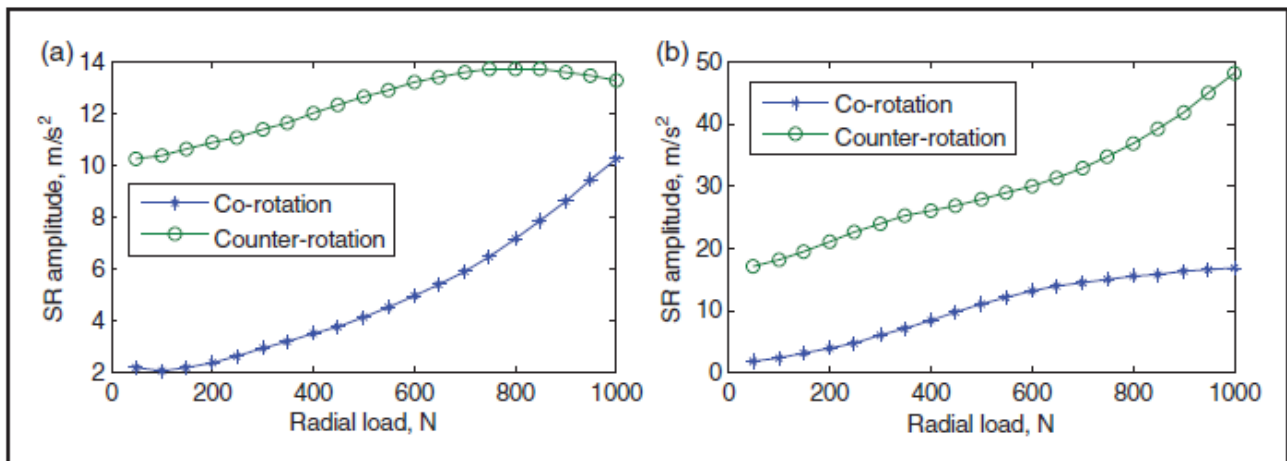


Figure 13. SR variation of bearing vibration signals under different loads on (a) outer and (b) inner race defects.

Tables.

Parameter	Value
Inner diameter, $\times 10^{-3}$ m	20
Outer diameter, $\times 10^{-3}$ m	42
Pitch diameter, $\times 10^{-3}$ m	31
Roller diameter, $\times 10^{-3}$ m	5.4
Number of rollers	13
Contact angle, $^{\circ}$	0
Radial clearance, $\times 10^{-6}$ m	12
Mass, kg	0.3
Damping coefficient, N s/m	200

Table 1. The parameters of the SKF nu1004M bearing.

Status	Passing frequency on inner race	Passing frequency on outer race
Co-rotation	47.17 Hz	33.55 Hz
Counter-rotation	145.3 Hz	206.7 Hz

Table 2. Passing frequency of inter-shaft bearing with defects.